Optical Engineering

SPIEDigitalLibrary.org/oe

Optical switch based on stimulated Raman scattering

Ariel Flores-Rosas
Evgeny A. Kuzin
Olivier Pottiez
Baldemar Ibarra-Escamilla
Manuel Duran-Sánchez

Optical switch based on stimulated Raman scattering

Ariel Flores-Rosas
Evgeny A. Kuzin
Instituto Nacional de Astrofísica
Optica y Electrónica
Luis Enrique Erro 1
Puebla, Puebla 72000 México
E-mail: aflores@inaoep.mx

Olivier Pottiez
Centro de Investigaciones en Óptica
León, Gto 37150, México

Baldemar Ibarra-Escamilla
Instituto Nacional de Astrofísica
Optica y Electrónica
Luis Enrique Erro 1
Puebla, Puebla 72000 México

Manuel Duran-Sánchez
Universidad Tecnológica de Puebla
Antiguo camino a la Resurrección 1002-A
Parque Industrial, Puebla, Puebla 72300 México

Abstract. We investigate optical switching based on stimulated Raman scattering. The circuit consists of two fiber stages connected in series through a bandpass filter. When the pump and signal are launched to the input, the pump is saturated because of the signal amplification in the first stage; the amplified signal is rejected by the filter, so that only low-power pump enters the second stage; and no signal pulses appear at the output. The second stage is fed by 1 mW power at signal wavelength. When the pump only enters at the input, it passes through the first stage without saturation, enters the second stage, and amplifies the signal entering this stage; strong signal pulses appear at the output. We use 2-ns pump pulses at 1528 nm and cw signal at 1620 nm. In the first stage, we use both fibers with normal and anomalous dispersion. In fibers with anomalous dispersion, pump saturation is affected by modulation instability. We find that the contrast may be improved using fibers with normal and anomalous dispersion connected in series in the first stage, provided there is appropriate selection of their lengths. The best contrast we achieve is 15 dB at 6 W pump peak power. [DOI: 10.1117/1.3558851]

Subject terms: fiber nonlinearities; optical signal processing; stimulated Raman scattering.

Paper 100444SSR received May 28, 2010; revised manuscript received Sep. 15, 2010; accepted for publication Oct. 13, 2010; published online Mar. 29, 2011.

1 Introduction

All-optical data-processing devices whose operation relies on nonlinear optical phenomena have attracted great interest in recent years as an alternative to electronic switching in optical communication systems. These devices have a strong potential for a variety of applications in such diverse areas as ultrahigh-speed optical telecommunications, ultrafast metrology, optical sensing, and optical computing. Advantages of processing the information in the all-optical domain include the very high potential bandwidth and the parallelism, which are not possible otherwise.[1,2] Multiple principles and devices were suggested. Among them a great part is embodied by devices based on the Kerr effect in fiber, such as a nonlinear optical loop mirror (NOLM) first proposed by Doran and Wood,[3] devices based on self-phase modulation (SPM) proposed by Mamyshev,[4] nonlinear couplers first discussed by Jensen,[5] devices using four-wave mixing (FWM) proposed by Ciaramella and Stefano,[6] and parametric amplification.[7] First reports were followed by numerous investigations proving the high performance of all-fiber devices. The NOLM was investigated for soliton switch,[8] signal regeneration with frequency repetition rate up to 160 GHz,[9] etc. On the applications of the NOLM, a comprehensive reference can be found in Ref. 10. The NOLM as well as other interferometric devices provide an oscillating power transfer function while the ideal characteristic is the steplike function. The power transfer function of the FWM-based devices approaches the steplike function; however, for a single-stage scheme, a flat response is achieved only at spaces while at marks an oscillating dependence was measured.[11] A double-stage scheme demonstrates flat response at both spaces and marks.[12] It was shown[13] that an optical regenerator that operates on the principle of a single power transfer function, such as the NOLM or FWM devices, does not improve a system's bit-error rate (BER) when placed just before the receiver and reduces the BER degradation from subsequent erbium-doped fiber amplifiers (EDFAs) stages. It was shown also that the regenerator based on SPM spectral broadening followed by filtering does improve the BER because it provides different power transfer functions for spaces and marks.[14]

There are only few works discussing the application of the stimulated Raman scattering (SRS) for signal regeneration and optical switch. However, SRS can be expected to present several advantages because of high amplification of the signal and intrinsic compatibility with communications systems employing Raman amplification of signals.[15] The design of Raman circuits can be based on the strong dependence of the Raman amplification on pump power that was considered for wavelength conversion with high extinction ratio.[16] With this approach, output signal pulses at Stokes wavelength are generated as a result of the Raman amplification caused by input signal pulses used as the pump. Because of the strong dependence of Raman amplification on pump power, the extinction ratio of the output signal can be much higher than that of the input signal. A second approach exploits pump saturation in presence of the signal.[17] In this case, the pulses at Stokes wavelength are used as an input signal, whereas the pump pulses are considered as an output signal. In the absence of the Stokes pulse (spaces), the pump pulse passes through the fiber without saturation and has high power at the fiber output (marks), whereas in presence of the Stokes pulse (marks) the pump pulse is depleted and has a low power at the fiber output (spaces). However, both approaches

0091-3286/2011/$25.00 © 2011 SPIE

do not provide a desirable steplike power transfer function. The combination of the Raman amplifier (where the pump is saturated by signals) and Raman amplifier (where the signal pulse is used as the pump) was also considered in connection with the recirculation loop, where the signal can travel in the closed fiber loop without degradation during an infinitively long time.[18] In this paper, we consider, theoretically and experimentally, the Raman circuit using the approach suggested in Ref. 18 and show that it allows the steplike power transfer function with high differential gain and low input signals. We find that the effect of modulation instability may degrade the operation of the device and show how this degradation can be avoided.

2 Basic Principles

In this section, we present simple numerical calculations to show the basic principles and potential of the approach. Figure 1 presents the basic diagram of the Raman circuit. It consists of two stages; each one may comprise several fiber spans. A wavelength division multiplexer WDM 1 serves to combine the pump and signal with Stokes wavelength in the first stage; WDM 2 serves to prevent entering of the Stokes signal to the second stage and to combine the pump and the seed at Stokes wavelength in the second stage. Stage 1 works as saturated amplifier where the pump pulses are saturated if the signal is at "marks" or travel through the fiber without saturation if the signal is at "spaces." Stage 2 works as a Raman amplifier with amplification, depending on the pump power entering from the first stage. If the input signal is at spaces, then the pump enters the second stage without saturation and generates high power at Stokes wavelength (i.e., the output signal is at Marks). If the input signal is at marks, then the pump is depleted in the first stage and the output signal is at spaces. Thus, the circuit operates as an inverter. For this operation to be allowed, the pump power has to be high enough to provide strong amplification of the signal and, simultaneously, lower than the SRS threshold at which strong Stokes pulses and pump depletion appears as a result of the amplification of the initial spontaneous Stokes waves. The wavelength shift between signal and pump must be close to the maximum Raman gain (~110 nm for the 1550-nm band). The wavelength of the cw seeding laser wave defines the wavelength of the output signal. It may not be the same as the wavelength of the input signal, which provides the possibility of wavelength conversion. Because of the large difference between pump and signal wavelengths, the walk-off between pump and Stokes is inevitable. To avoid the degradation of the operation because of the walk-off effect, dispersion management can be used to connect fibers in which the signal travels faster than pump to fibers in which the signal travels slower than pump. If fibers with anomalous dispersion are used however, then modulation instability (MI) can be expected, which will complicate drastically circuit operation.

As the first step, to illustrate the operation principle, we evaluated the Raman circuit on the basis of the coupled equation for pump, A_P, and Stokes, A_S, pulses,

$$\frac{\partial A_S(t)}{\partial z} + (1/V_P - 1/V_S)\frac{\partial A_S(t)}{\partial t} + i\frac{\beta_2}{2}\frac{\partial^2 A(T,z)}{\partial t^2} = \frac{g}{2}A_S(t)\,|A_P(t)|^2$$

$$\frac{\partial A_P}{\partial z} + i\frac{\beta_2}{2}\frac{\partial^2 A_P(T,z)}{\partial t^2} = -\frac{g}{2}A_P\,|A_S|^2 \qquad (1)$$

where g is the Raman gain coefficient, V_P and V_S are the group velocity of pump and Stokes, respectively, and β_2 is group velocity dispersion (GVD). Here, we do not consider the effects connected with nonlinear Kerr effect to provide the simplest explanation of the basic principles. However, this effect may be important, especially in fibers with anomalous GVD, because it may cause the modulation instability and pulse breakup. We calculated the energy of the input Stokes pulse at the output of the circuit depending on the power of the Stokes power at the input of the first stage. The calculations were done with the split-step Fourier method with $g = 0.6 \times 10^{-13}$ m/W corresponding to the Raman gain maximum for pump wavelength of 1550 nm,[19] input pump pulse duration of 100 ps and power of 15 W, and effective area of fibers of 50 μm^2. Three types of fibers with different GVD were used: Fiber 1 with $D = -6$ ps/(nm-km); fiber 2 with $D = 20$ ps/(nm-km); fiber 3 with $D = -0.01$ ps/(nm-km). The dispersions of fibers 1 and 2 correspond to the dispersions of the Corning dispersion-shifted fiber SMF-LS and Corning SMF-28 fiber at 1550 nm. Fiber 3 represents some fiber with no walk-off between the pump and Stokes pulses. We used this fiber in calculation to show how the effect of walk-off affects the performance of the Raman circuit. The fulfillment of this condition depends on the relation between fiber length, pulse length, and fiber dispersion.

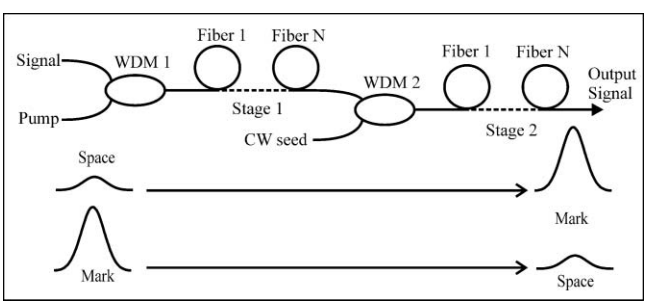

Fig. 1 Principle diagram of the Raman circuit.

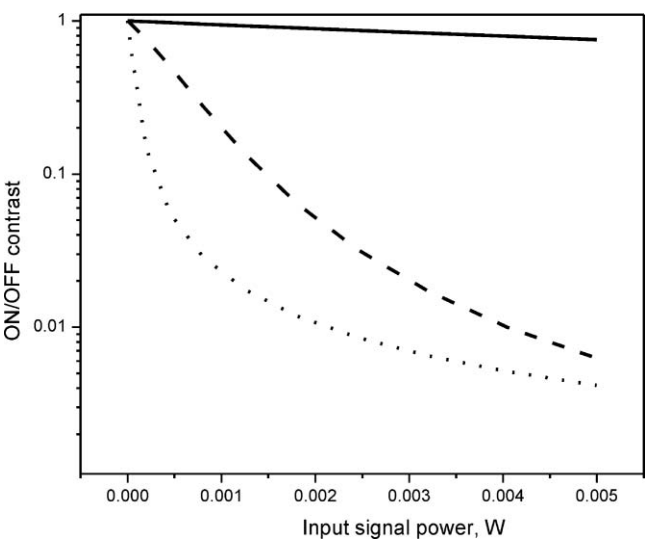

Fig. 2 Energy of Stokes pulses at the output of the circuit.

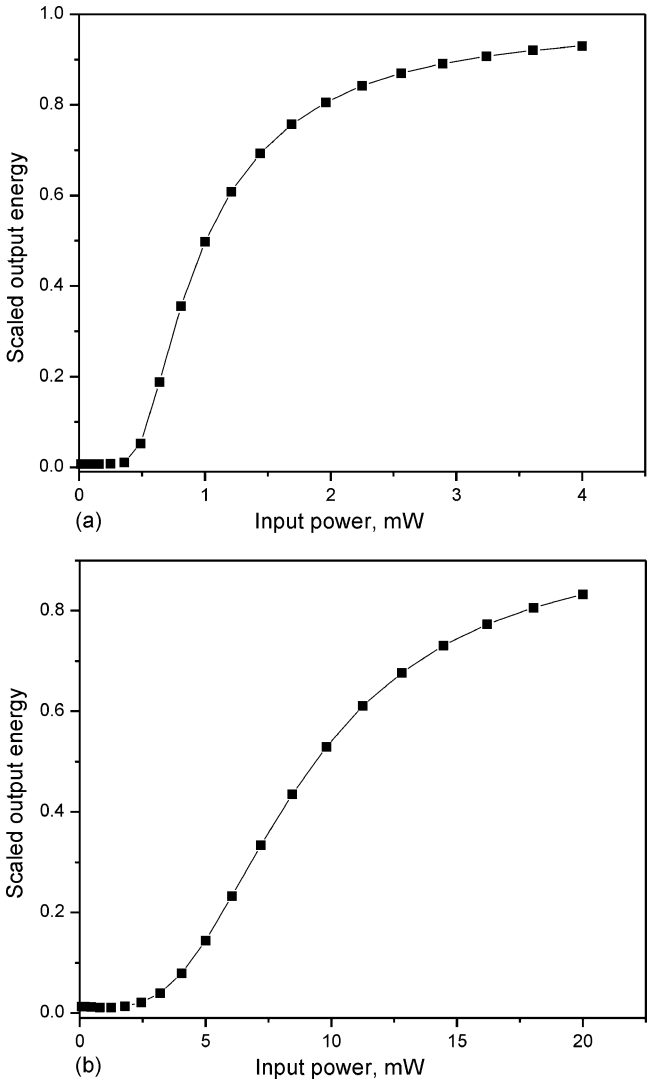

Fig. 3 Dependencies of the output Stokes energy on the input power for two Raman circuits connected in series: (a) attenuation between the circuits is 10 times and (b) attenuation between the circuits is three times.

The dependencies of the energy of the output signal pulse on the input signal power are presented in Fig. 2 for three different configurations of stage 1. The energy is scaled with respect to the energy of the output signal when no signal enters from the input. The solid line represents the switch when stage 1 comprised only fiber 1 of 295 m in length. The dashed line represents the case when stage 1 comprised three fibers connected in series: 150 m of fiber 1, 45 m of fiber 2, and 100 m of fiber 3. The dotted line shows the results when the first stage comprised 295 m of fiber 3. For all cases, 350 m of fiber 3 was used for stage 2. As we expected, the result depends drastically on the walk-off. The best result is provided by the fiber with low dispersion. In practice, it may not be very easy to fulfill the condition that the walk-off length be longer than the fiber length, especially if low power and, thus, a long fiber is required. However, a simple dispersion-management technique using only three lengths of fibers with normal and anomalous dispersion may provide switching with a contrast (the ratio between the energies of the signals at the second stage output when the input signal is spaces and marks) of ~20 dB at input power of $<10^{-3}$ of pump power.

Two successive circuits provide the steplike dependence. Figure 3(a) shows the dependence for two circuits connected in series corresponding to the dotted line in Fig. 2. Figure 3(b) shows the dependence for two circuits corresponding to the dashed dependence of Fig. 2. The characteristics depend on the attenuation between circuits. For particular cases shown in Fig. 3, the attenuation is 10 times for Fig. 3(a) and three times for Fig. 3(b).

The simple presented considerations show that the Raman circuit allows effective optical switching, logic operation, and noise reduction with signal power as low as 10^{-3} of the pump power. However, there are several effects that will affect the Raman circuit operation and must be considered. As we have seen, the connection in series of fibers with normal and anomalous dispersions allows a strong improvement of the operation of the circuit. However, in fibers with anomalous GVD, the effect of MI and pulse breakup appear at powers lower than that required for strong Raman amplification.[20] It can be expected that pulse breakup will affect the depletion of the pump pulse and amplification of the Stokes pulses. Only few works addressed this problem, mostly related to the generation of supercontinuum and Raman amplification of signals.[21]

The principal characteristics of the circuit are the pump pulse duration and power, and the signal pulse duration and power. The delay time, depending on the fiber length, indeed does not affect the bandwidth of the circuit. The principal limit of the pulse duration is defined by the response time of the Raman effect and lies in the femtosecond scale. However, for reasonable pump powers and fiber parameters, the limit of the pulse duration is defined by the walk-off between pump and signal rather than by the response time. We numerically show the operation for 100-ps pulses and fiber parameters corresponding to widely available fibers. However, the development of the photonics crystal fibers allows fabrication of the fibers with very high flexibility of the dispersion characteristic and nonlinear properties. The use of pulses with several picoseconds of duration and <1 W of power can be easily expected.

3 Experimental Results

The experimental setup is presented in Fig. 4. Our experimental system used as a source of pump pulse, a diode laser with $\lambda = 1528$ nm. This diode laser is directly modulated by the pulse generator SRS DG535 to generate pulses with duration of 2 ns. The pulses from the diode laser with power of several megawatts are amplified by an EDFA to the power of several tens of watts. A detailed description of the EDFA can be found in Ref. 22. As an input signal, we used a cw laser diode with wavelength of 1620 nm. The pump pulses and input signal are introduced to the 85/15 coupler 1

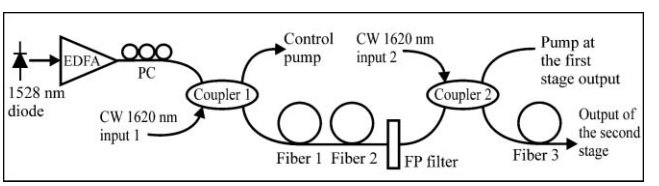

Fig. 4 Experimental setup.

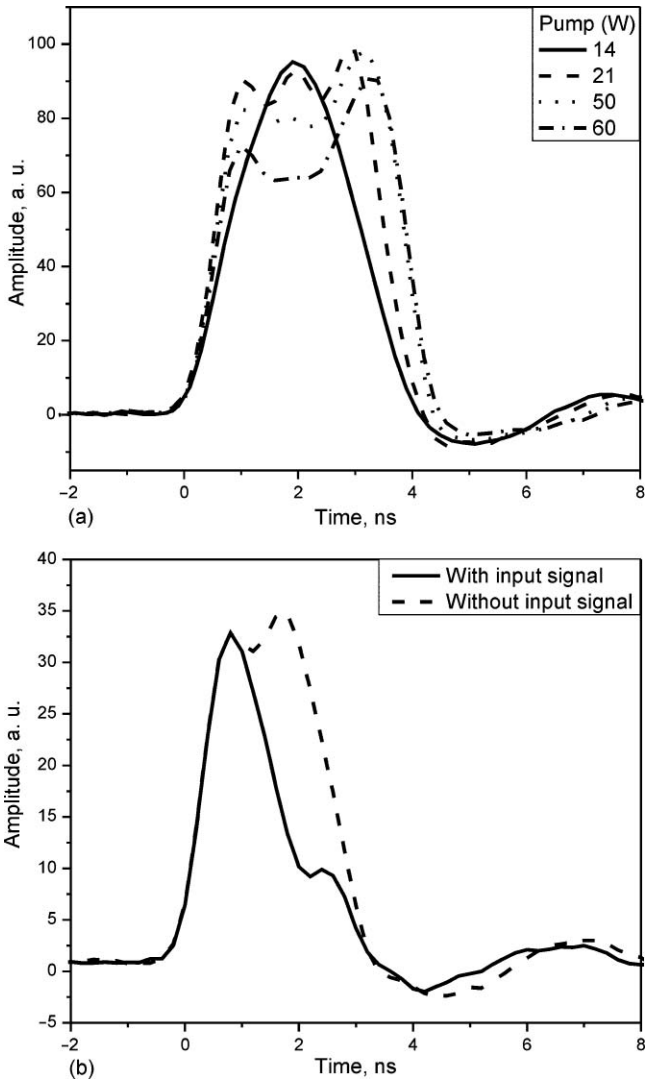

Fig. 5 Pump pulses at the output of the FP filter when the SMF-28 fiber was used as fiber 1: (a) Fiber length is equal to 200 m and (b) fiber length is equal to 1 km.

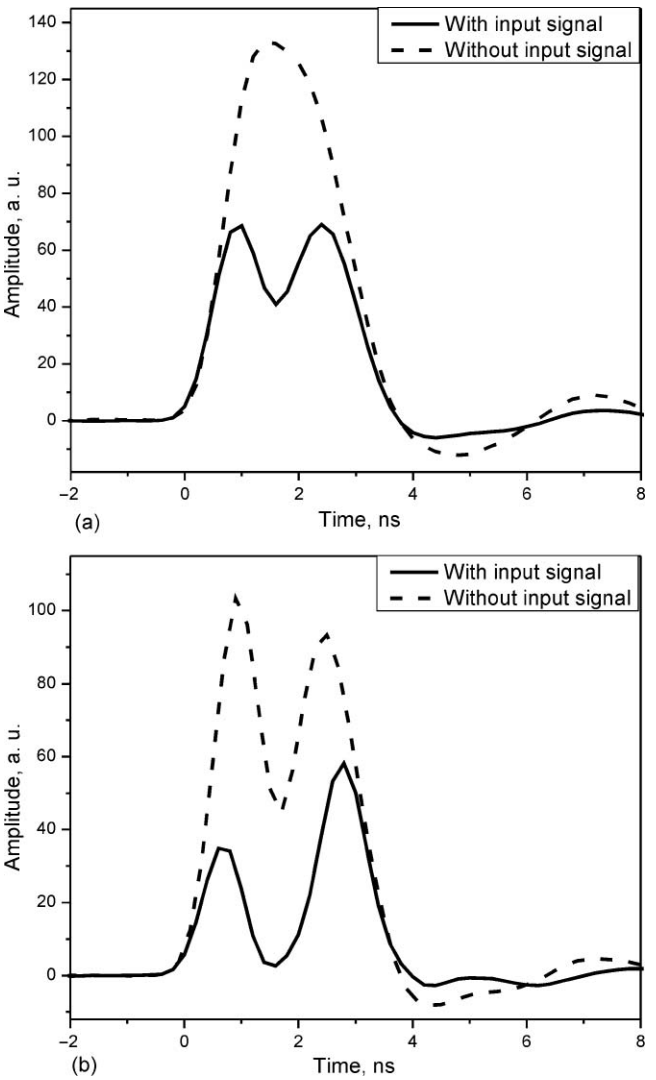

Fig. 6 Saturation of the pump by the input signal with 550 m of SMF-LS fiber: (a) for 20 W and (b) for 25 W of pump power.

that serves to combine pump and signal. Coupler 1 couples to fiber 1 85% of the pump power and 15% of the signal. The power of the signal launched to the fiber was 0.5 mW; the power of the pump can be changed in an approximate range between 1 and 50 W. In the first stage, we used either dispersion-sifted SMF-LS fiber or SMF-LS (fiber 1) connected in series with SMF-28 fiber (fiber 2). The fiber SMF-28 has anomalous GVD equal to 20 ps/(nm-km), and the fiber SMF-LS has a normal dispersion equal to –6 ps/(nm-km) at 1550 nm. The polarization controller inserted after the EDFA allows adjusting the polarization of the pump to provide a maximum Raman amplification in the fibers because the Raman amplification depends on polarization states of pump and Stokes.[23,24] The Fabry–Pérot (FP) filter was used to reject the 1620 nm radiation at the end of the first stage. The transmission of the FP filter for 1528 nm radiation was –4 dB. The 90/10 coupler 2 was used to combine the 1528-nm pump pulses and 1620-nm cw signal in the second stage of the Raman circuit. The signal power launched into fiber 3 was ~0.5 mW. The use of coupler 1, the FP filter, and coupler 2 instead of WDMs (shown in Fig. 1) causes a significant loss of pump and signal powers; however, this schematic allows the investigation of the circuit operation in the absence of the convenient WDMs. As fiber 3, we used 4.5 km of OFS True Wave (RS) fiber. With this configuration, we were able to simultaneously measure the pump pulse at the input of the first stage, the pump at the output of the first stage, and the Stokes or pump pulses at the output of the second stage. The pulses at the output of the second stage were detected using a monochromator, a 1-GHz InGaAs photodetector, and a 500-MHz oscilloscope. The pump pulses at the output of the EDFA were detected by a 10-GHz InGaAs photodetector and a 20-GHz sampling oscilloscope.

As can be seen from the simulation, the process of the pump saturation in the first stage is very important for the circuit operation. We investigated the pump saturation in the first stage for different lengths of fibers 1 and 2. Figure 5 presents the waveforms of pump pulses at the output of the FP filter for different pump powers when only fiber 1 was used in the first stage. Figure 5(a) was obtained with a fiber length of 200 m and Fig. 5(b) with fiber length of 1 km. Strong depletion of the pump pulse was observed for the 200-m fiber even if the 1620-nm radiation was not applied. In this case,

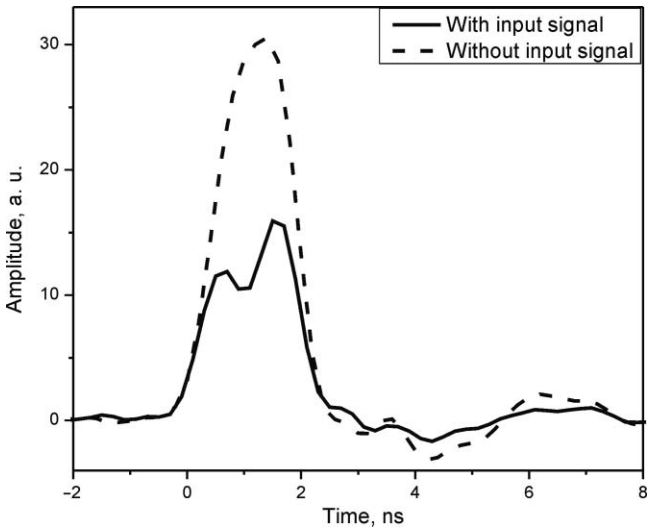

Fig. 7 Saturation of the pump by the input signal if the first stage comprises a 550-m SMF-LS fiber connected to a 300-m SMF-28; pump power is 21 W.

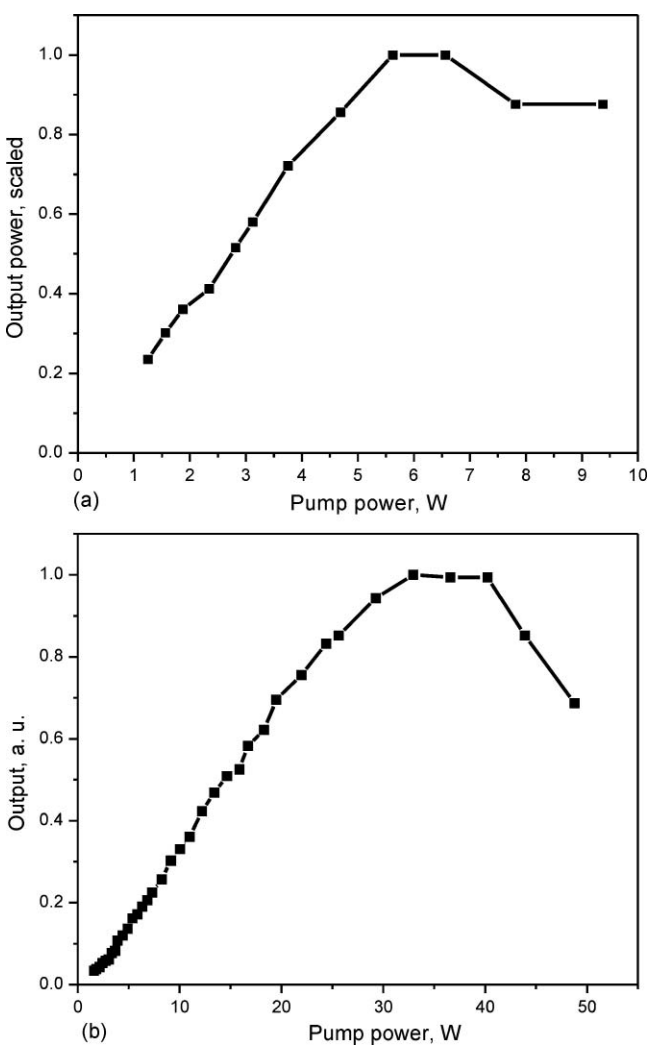

Fig. 8 Saturation of pump measured with narrowband and broadband filter.

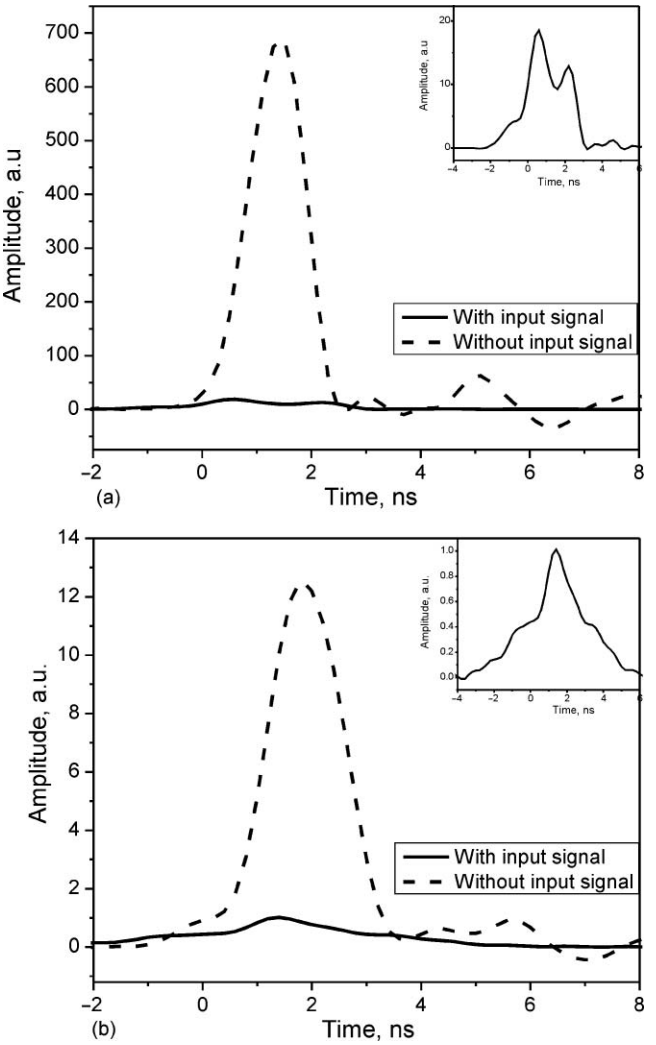

Fig. 9 Waveforms of the signal at 1620 nm at the output of fiber 3: input signal is off (dashed line), input signal is on (solid line). Insets show the magnifications of the output signal when input signal is on. (a) The first stage consists of the 350 m of the SMF-LS fiber and (b) the first stage consists of the 350-m SMF-LS connected to the 600-m SMF-28.

the effect of the 1620-nm radiation on the pulse depletion was not detected. The maximum power at the FP output was measured to be equal to 8 W. The pump depletion is caused by the pulse breakup process followed by the soliton self-frequency shift, which results in broadening of the spectrum and a decrease of power at the output of the FP filter. For the 1-km fiber, the depletion caused by the pulse breakup also was observed; however, some effect of the 1620-nm radiation was detected.

The experiment using the SMF-LS fiber with normal dispersion shows conventional saturation of the pump that corroborates well the simulations based on Eq. (1). Figure 6 presents the results for a fiber of 550 m in length. At pump power equal to 20 W [Fig. 6(a)], without an input signal, no change in the waveform of the pump pulse is observed. However, at 0.5 mW of signal input power, strong depletion can be seen. At 25 W of pump power, the depletion is observed even without input signal [see Fig. 6(b)]. In this case, a strong Stokes pulse at 1635 nm was detected that causes the pump depletion. In conventional terms, this means that the pump

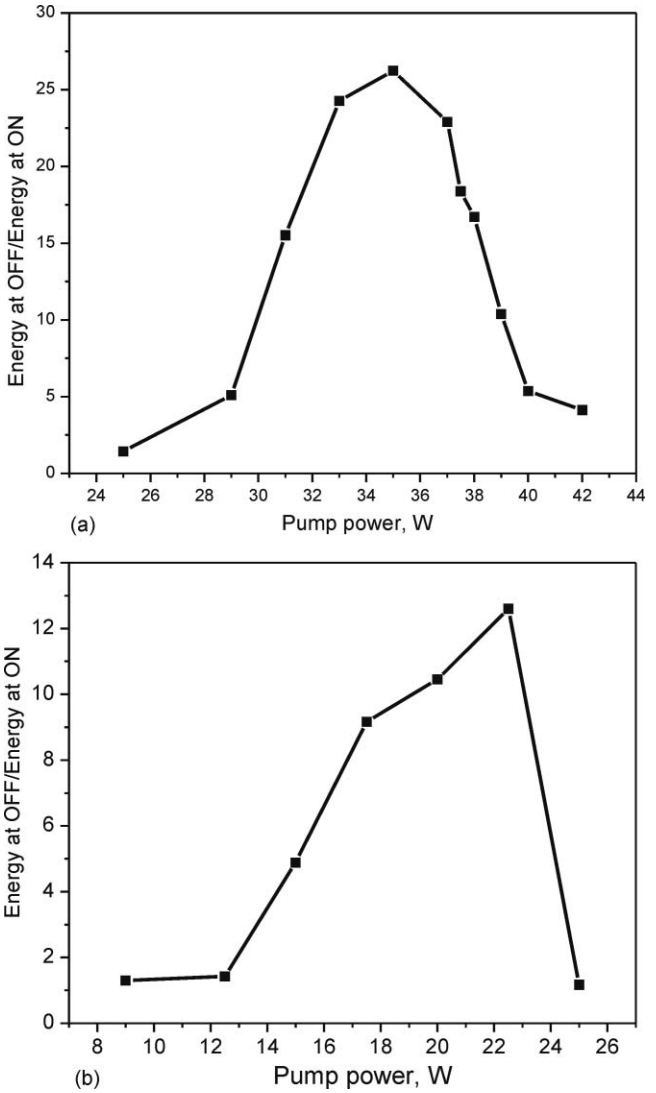

Fig. 10 Energy of Stokes pulses: (a) for 350 m SMF-LS in the first stage and (b) for 350 m SMF-LS + 600 m SMF-28 in the first stage.

power is higher than the threshold power. However, in this case, a strong effect of the input signal can still be seen.

The composed fiber consisting of the span of SMF-LS spliced with the span of SMF-28 was also tested. The saturation of the pump by input signal was observed if the length of SMF-LS is at least two times longer than the length of the SMF-28. In this case, the power required for MI is higher than that required for effective pump depletion. Figure 7 presents an example of the output pump pulses at the end of the first stage, which consisted from a 550-m span of SMF-LS and a 300-m span of SMF-28. However, the effect of GVD in SMF-28 on the pulse waveform and pump saturation is not significant for 2-ns pulses.

If the pump depletion in the first stage composed from the SMF-28 is determined by MI, then the results of the depletion must be dependent on the bandwidth of the filter inserted between the first and second stages. To prove this, we used as a broadband filter and a span of the SMF-28 coiled up on a cylinder with a diameter of 16 mm. For a small radius of curvature, a strongly wavelength-dependent loss appears. For our case, the loss of the fiber with curvature was measured to be 18 dB for 1620 nm and 5.5 dB for 1528 nm. The difference between losses is sufficient to measure the depletion of the pump with this broadband filter. Figure 8(a) represents the results of the depletion measurement with the FP filter with bandwidth of 1 nm, and Fig. 8(b) with the broadband filter. It can be clearly seen that, with the narrowband filter, the pump depletion appears at ∼5 W of pump power; whereas with the broadband filter, the pump depletion appears at 30 W of input power. These results show that the problem connected with the MI could be overcome using the broadband filter between the first and second stages. It could be, for example, a filter based on a liquid-filled photonic crystal fiber[25] with steplike dependence of transmission on the wavelength.

Finally, we tested the two-stage setup. In the second stage, we used a 4.5-km OFS True Wave (RS) fiber. In the first stage, we used different combinations of the dispersion-shifted Corning SMF-LS fiber and Corning SMF-28 fiber. Figure 9 shows examples of the waveforms of the signal pulses at the output of fiber 3. The results of Fig. 9(a) were obtained with 350 m of SMF-LS as the first stage at 37 W of pump power; the results of Fig. 9(b) were obtained with 550 m of SMF-LS spliced with 600 m of SMF-28 used as the first stage at 21 W of pump power. The insets show the magnifications of the output signal when input signal is applied.

Figure 10 shows the dependencies of the contrast on the pump power. The contrast was measured as the ratio between the energies of the signals at the second stage output when the input signal is turned off and on. The dependencies are shown for the first stage, consisting of the 350-m SMF-LS fiber [Fig. 10(a)], and for the first stage consisting of the 350-m SMF-LS and the 600-m SMF-28 fiber [Fig. 10(b)].

4 Conclusions

The use of SRS to design an all optical switch circuit makes it possible to use very low powers of signal to control respectively strong pulses. The principle of operation can be based on pump depletion because of the transference of energy from the pump to the first Stokes. The pump depletion and, respectively, the on-off contrast are restricted by pulse shape and GVD. We investigated a two-stage setup and the dispersion management technique to improve the on-off contrast, and have experimentally obtained the contrast equal to 15 dB for a signal power as low as 0.5 mW. We have found that the pump depletion in fibers with anomalous dispersion is deteriorated by the pulse breakup process; thus, the use of the dispersion-management technique requires the appropriate selection of fibers with anomalous and normal dispersion.

Acknowledgments

The authors thank the Mexican Council for Science and Technology for providing financial support by the CONACyT Project No. 47169.

References

1. O. Leclerc, B. Lavigne , E. Balmefrezol, P. Brindel, L. Pierre, D. Rouvillain, and F. Seguineau, "Optical regeneration at 40 Gb/s and beyond," *J. Lightwave Technol.* **21**(11), 2779–2790 (2003).
2. G. I. Papadimitriou, C. Papazoglou, and A. S. Pomportsis, "Optical switching: switch fabrics, techniques, and architectures," *J. Lightwave Tech.* **21**(2), 384–405 (2003).
3. N. J. Doran and D. Wood, "Nonlinear-optical loop mirror," *Opt. Lett.* **13**(1), 56–58 (1988).

4. P. V. Mamyshev, "All-optical data regeneration based on self-phase modulation effect," in *Proc. of 1998 Eur. Conf. Optical Commun.*, pp. 475–476 (1998).
5. S. M Jensen, "The nonlinear coherent couplers," *IEEE J. Quantum Electron.* **QE-18**(10), 1580–1583 (1982).
6. E. Ciaramella and T. Stefano, "All-optical signal reshaping via fourwave mixing in optical fibers," *IEEE Photon. Technol. Lett.* **12**(7), 849–851 (2000).
7. S. Radic, C. J. McKinstrie, R. M. Jopson, J. C. Centanni, and A. R. Charplyvy, "All-optical regeneration in one- and two-pump parametric amplifiers using highly nonlinear optical fiber," *IEEE Photon. Technol. Lett.* **15**(7), 957–959 (2003).
8. M. N Islam, C. E Soccolich, and D. A. B Miller, "Low energy ultrafast fiber soliton logic gate," *Opt. Lett.* **15**(16), 909–911 (1990).
9. A. Bogoni, P. Ghelfi, M. Scaffardi, and L. Potì, "All-optical regeneration and demultiplexing for 160-Gb/s transmission systems using a NOLM-based three-stage scheme," *IEEE J. Sel. Top. Quantum Electron.* **10**(1), 192–196 (2004).
10. S. Boscolo, S. K. Turitsyn, and K. J. Blow, "Nonlinear loop mirror-based all-optical signal processing in fiber-optic communications," *Opt. Fiber Technol.* **14**(4), 299–316 (2008).
11. E. Ciaramella, F. Curti, and S. Trillo, "All-optical signal reshaping by means of four-wave mixing in optical fibers," *IEEE Photon. Technol. Lett.* **13**(2), 142–144 (2001).
12. S. Yamashita and S. Mazumder, "Optical 2R regeneration using cascaded fiber four-wave mixing with suppressed spectral spread," *IEEE Phot. Tech. Lett.* **18**(9), 1064–1066 (2006).
13. M. Rochette, J. N. Kutz, J. L. Blows, D. Moss, J. T. Mok, and B. J. Eggleton, "Bit-error-ratio improvement with 2R optical regenerators," *IEEE Photon. Technol. Lett.* **17**(4), 908–910 (2005).
14. M. Rochette, J. L. Blows, and B. J. Eggleton, "3R optical regeneration: an all-optical solution with BER improvement," *Opt. Express* **14**(14), 6414–6427 (2006).
15. C. Headley and G. P. Agrawal, *Raman Amplification in Fiber Optical Communication Systems*, Elsevier Academic Press, New York (2005).
16. A. Uchida, M. Takeoka, T. Nakata, and F. Kannari, "Wide-range all-optical wavelength conversion using dual-wavelength-pumped fiber Raman converter," *Lightwave Tech.* **16**(1), 92–99 (1998).
17. F. Ahmed and N. Kishi, "All-fiber wavelength conversion of ultra-fast signal with enhanced extinction ratio using stimulated Raman scattering," *Opt. Rev.* **10**(1), 43–46 (2003).
18. V. I. Belotitskii, E. A. Kuzin, M. P. Petrov, and V. V. Spirin, "Demonstration of over 100 million round trips in recirculating fiber loop with all-optical regeneration," *Electron. Lett.* **29**(1), 49–50 (1993).
19. G. P Agrawal, *Nonlinear Fiber Optics*, Academic Press, New York (2001).
20. R. Rojas-Laguna, J. Gutierrez-Gutierrez, E. A. Kuzin, M. A. Bello-Jimenez, B. Ibarra-Escamilla, J. M. Estudillo-Ayala, and A. Flores-Rosas, "Nonlinear optical correction of the pulse shape from a directly modulated DFB laser," *Opt. Commun.* **281**, 824–830 (2008).
21. A. E. El-Taher, J. D. Ania-Castañón, V. Karalekas, and P. Harper, "High efficiency supercontinuum generation using ultra-long Raman fiber cavities," *Opt. Express* **17**(20), 17909–17915 (2009).
22. M. A. Bello-Jimenez, E. A. Kuzin, B. Ibarra-Escamilla, and A. Flores-Rosas, "Optimization of the two-stage single-pump erbium-doped fiber amplifier with high amplification for low frequency nanoscale pulses," *Opt. Eng.* **46**(12), 125007 (2007).
23. Q. Lin and G. P. Agrawal, "Vector theory of stimulated Raman scattering and its application to fiber-based Raman amplifiers" *J. Opt. Soc. Am.* **B20**, 1616–1631 (2003).
24. S. Sergeyev, S. Popov, and A. T. Friberg, "Modeling polarization-dependent gain in fiber Raman amplifiers with randomly varying birefringence," *Opt. Commun.* **262**, 114–119 (2006).
25. S. Torres-Peiró, A. Díez, J. L. Cruz, and M. V. Andrés, "Fundamental-mode cutoff in liquid-filled Y-shaped microstructured fibers with Ge-doped core," *Opt. Lett.* **33**(22), 2578–2580 (2008).

Biographies and photographs of the authors not available.